The 2012 World Congress on
Advances in Civil, Environmental, and Materials Research (ACEM' 12)
Seoul, Korea, August 26-30, 2012

Uniform flow around a square cylinder using the Self-induced angular Moment Method turbulence model

*Johansson, Jens[1)], Nielsen, M. P.[2)], Nielsen, Leif O.[3)]
[1)]*Institute of Technology and Innovation, University of Southern Denmark, Campusvej 55 5230 Odense M, Denmark*
[1) 2)] *Alectia A/S, Teknikerbyen 34, 2830 Virum, Denmark*
[2),3)] *Department of Civil Engineering, Technical University of Denmark, Anker EngelundsVej 1, 2800 Kgs. Lyngby, Denmark*
[1)] *jensj@iti.sdu.dk*

ABSTRACT

The uniform flow around a square cylinderat Reynolds number 1e5 is simulated in a three-dimensional domain by means of the newly developedSelf-induced angular Moment Method, SMoM.The model does not utilize Reynolds averaging. No additional transport equations are introduced and no implicit or explicit filtering is performed. The model is, in all its simplicity, a modification of the classical constitutive equations of fluids to which a term is added that accounts for the transfer for angular momentum between parts of the fluid.
The time-mean and fluctuating force coefficients, pressure distributions and velocity fields have been determined along with circumferential surface pressure correlations. All simulated quantities have been compared to experimental findings and state-of-the-art Large Eddy Simulations, LES. No LES simulations could be found in literature, which provided results at the same level of accuracy for all the reported parameters. Hence, the SMoMturbulence model is found to provide an alternative to the Large Eddy Simulations.

1. INTRODUCTION

The flow around a square cylinder obviously involves very simple geometry in a civil engineering context. However, the flow around the square cylinder is highly complex. For this reason the flow over a square cylinder has previously been used as a test case for Large Eddy Simulations. The flow was chosen as a test case at a workshop in Rottach-Egern, Germany in the summer of 1995. The findings from the workshop were published in (Rodi et. al 1997). Ten different groups submitted a total of sixteen sets of results. As there were a large variation of numerical methods it was difficult to evaluate the actual performance of the individual method. Unfortunately, this lead to the somewhat weak conclusion that "no conclusion could be made on the effect of choice of numerical method". This was later addressed by (Nakayama and Vengadesan 2002). No single set of results was highlighted, and the results of the workshop

[1)]Ph.D. candidate
[2)] Dr.techn., Professor Emeritus, Technical University of Denmark and permanent consultant at Alectia A/S
[3)] Associate Professor Emeritus

were concluded with; “Overall, it is our judgment that no single simulation is uniformly good; significant faults can be found in every submission”.
In September 1996 the flow around a square cylinder was also adopted for the Second ERCOFTAC Workshop on Direct and Large-Eddy Simulation held in Grenoble, France. The proceedings of this workshop were published in (Voke 1997). Here seven groups of researchers submitted a total of 20 data sets, of which a selection was compared in (Voke1997). Grid convergence was considered in some of the submitted data sets, though it was stated that none had demonstrated convergence convincingly. It was noted that the simultaneous prediction of the recirculation length and the recovery of the centerline velocity was very difficult, as was also noted in the (Rodi et al. 1997) workshop. One group defied this rule, and predicted both.However, their reported drag coefficient was not reassuring. The NT7 submission was highlighted as this simulation predicted most of the integral parameters correctly, though there were some discrepancies in the velocity field. The force coefficients predicted by this group are provided in Table 2. The final conclusion at the (Rodi et al. 1997) workshop was consistent with previous findings; “The flow over and following the square cylinder is therefore proving a major challenge to current LES techniques, a stimulus to further investigation and a problem to which, at present, we cannot claim to have a definitive solution.”.
(Lee and Bienkiewicz1998) performed 2D and 3D LES simulations at $Re = 22000$ usingisoparametric elements in aGalerkin FEM discretization. The standard Smagorinsky model was employed using $C_s = 0.1$. The global force statistics were well predicted, as seen in Table 2. However the velocity profiles downstream of the cylinder were over predicted, also causing a slight over prediction of the recirculation length. The time-mean pressure distribution agreed well with the pressure distribution reported by (Murakami and Mochida 1995) who used a dynamic Smagorinsky model, and also agreed well to the experimental findings by (Bearman and Obasaju1982).
(Sohankar et al. 2000) later performed six different simulations using three different sub-grid scales models. One simulation was performed with each of the Standard Smagorinsky ($C_s = 0.1$) and the dynamic Germano-Lilly model. The remaining four simulations were performed with a dynamic one-equation model developed by Davidson. See (Sohankar et al. 2000). Blockage corrected results of one of the simulations were presented, which agreed very well with the corrected global quantities from experiments. The effect of span-wise length was investigated. The fluctuating drag were reduced by 6% by extending the cylinder length from four to seven side lengths, while other quantities were within $\pm 2\%$. For an increase in time resolution by a factor 2 the only significant change was a 5% reduction of the fluctuating drag. Further the rmsquantities $(\overline{u'u'})^{1/2}$, $(\overline{v'v'})^{1/2}$ in the centerline were very well predicted. However, the peak in $(\overline{v'v'})^{1/2}$ occurred early as was also mentioned in (Voke 1997), and the cross sectional profiles of velocity variances (rms squared) showed some deviation from the experimental findings for one of their downstream locations. The reported recirculation length was smaller than the experimental, and the velocity in the recirculation zone was not found to be as negative.

In the present paper the case of flow around a square cylinder illustrated in Fig. 1will be used to assess the performance of the SMoM turbulence model.We consider a square cylinder of side length d and a span-wise length $l = 2d$ in the z-direction. The cylinder is subjected to turbulence-free incoming stream of a velocity u_∞ in the x-direction. The dimensions of the computational domain are given the cross-stream height $H = 20d$in the y-direction and stream-

wise length $L = 40d$, with the inlet plane placed an upstream distance of $10d$ from the cylinders center of gravity.

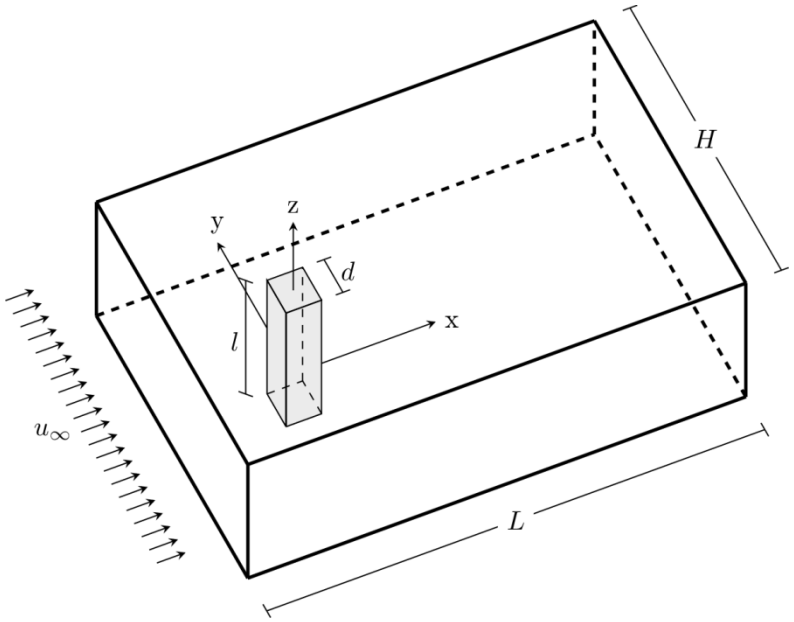

Fig. 1. – Principal orientation of the square cylinder in thecomputational domain.

2. THE SMoM TURBULENCE MODEL

The SMoM turbulence model has been suggested by (Nielsen et al 2006). The model was further calibrated and boundary conditions were developed in (Johansson, J. 2011). A short introduction to the model is offered here.
If we let the axis x_1, x_2, and x_3 define a right-hand coordinate system, then theNavier-Stokes equation in continuity form, with zero body forces, may be written in index notation as in Eq. (1).

$$\rho \frac{\partial u_i}{\partial t} + \rho \frac{\partial}{\partial x_j}\left(u_j u_i\right) = \frac{\partial \tau_{ji}}{\partial x_j} \tag{1}$$

where$t$ is time, ρ is density, u_i is the velocity vector,and τ_{ij} is the Cauchy stress tensor.The SMoM turbulence model is a zero equation turbulence model in the sense that no additional transport equations are introduced. The model is merely a modification of the constitutive equation of the Newtonian fluid. For the Newtonian fluid the classical terms takes into account the transfer of linear momentum between parts of the fluid. In the SMoM turbulence model a term is added which takes into account the transfer for angular momentum between parts of the fluid. Thus the constitutive equation of the fluid reads

$$\tau_{ij} = -p\delta_{ij} + 2\mu d_{ij} + 2bu^{\alpha}\Omega_{\mathrm{ji}} \tag{2}$$

whered_{ij} is the strain rate tensor, δ_{ij} is Kroneckerdelta, μ is the dynamic viscosity, and p is the pressure. The first two terms completes the usual constitutive equation for the Newtonian fluid. The term $2bu^{\alpha}\Omega_{\mathrm{ji}}$is thus the added term, where$\Omega_{\mathrm{ji}} = 1/2\left(\partial u_i/\partial x_j - \partial u_j/\partial x_i\right)$ is the rate-of-rotation tensor, b is the local value of SMoM models scale parameter and $u^{\alpha}$is the absolute velocity $\sqrt{u_i u_i}$ to the power of α, which is a model parameter. The local value of b is given by boundary conditions and the base value of the scale parameter,b_0, whichin the case of smooth walls may be determined from

$$b = k_1\left(\frac{\mu}{\rho}\right)^{1-\alpha} {r_p}^{\alpha}\rho \tag{3}$$

The value of the model parameters$k_1 = 0.0158$and $\alpha = 0.8482$ have been determined from a least square fit of analytical velocity profiles in smooth pipes to the experimental data in (Nikuradse 1932). The constant $r_p^{\alpha}$is labeled the *scale factor*, which is not a fluid property, but rather a flow property. The *scale factor* represents a characteristic length-scale in the simulated flow. In the case external flow around a square cylinder we set the lengthr_p equivalent to the cylinder side length d.

3. SIMULATIONS

The simulations have been performed using the open source software package OpenFOAM version 1.6.x, which is based on the Finite Volume Method. An existing implementation of the PISO solution method was used through a modification of an existing solver. The Crank-Nicholson scheme was used for temporal discretization. For the spatial discretization second order central differencing was used, while a built-in Total Variation Diminishing, TDV, scheme was used for the convective terms.

At the outlet boundary a built-in *advective* boundary condition was used, which is based on $du_i/dt + u_\infty\, du_i/dx = 0$. For the upper, lower, and cylinder-end boundaries a symmetry boundary condition was used.At the cylinder surface the no-slip condition was enforced, and the scale parameter$b$ was given a linear variation with the distance to the wall within a zone around the square extending to an absolute distance of $y_T = 0.2d$ away from the surface. Hence at the surface of the cylinder $b = 0$ while $b = b_0$ at, and beyond the transition point y_T .In the implementation of theSMoM model the scale parameter b was considered to be a local constant in the sense that the scale parameter b was moved outside the differentiation indicated in Eq. (1). With this rather crude handling of the boundary conditions an accurate determination of the surface shear stresses cannot be expected. Hence, further work on the boundary conditions is still in progress. The computational grid was structured according to the general layout outlined inFig. 2, with a grid refinement zone with a diameter of $5d$. Three different computational grids were used; Grid A, B and C. The grids were designed as structured grids based on the number of cells listed in Table 1.

Grid	N_{in}	N_{out}	N_{up}	N_z	D/d	N_i	R_i	N_{tan}	$Cells$
A	20	75	20	20	2.5	21	10	10	119,800
B	40	150	40	40	2.5	43	10	20	961,600
C	40	150	40	40	2.5	86	10	40	1,590,400

Table 1. Table of grid definitions. The definitions of N_x and R_i are given in Fig. 2.

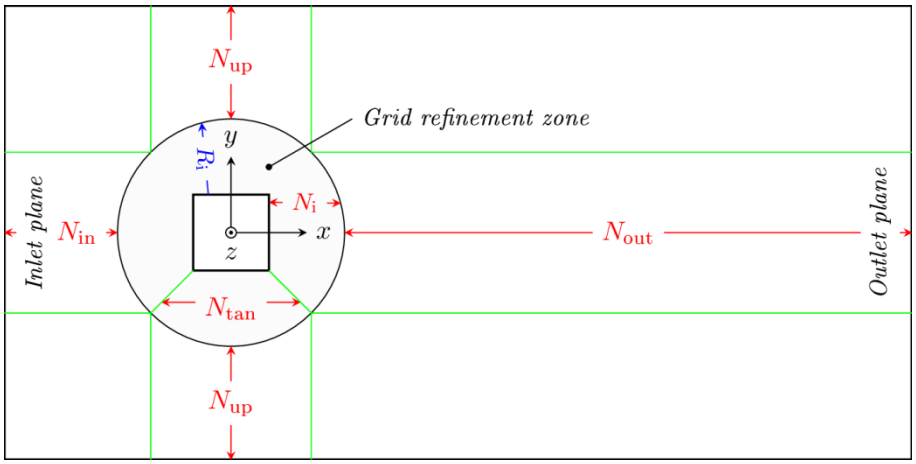

Fig. 2. – Principal structure of the computational grid. $N_x$designates the number of cells in the indicated directions. $R_i$indicates the expansion ratio in the indicated direction.

4. RESULTS AND DISCUSSION

Simulations were allowed to reach a “stable” condition before any results were collected. The results presented here are based on a non-dimensional time interval of minimum $\Delta t u_\infty/d = 400$ .Both spatial and temporal convergence has been considered. The time-mean force coefficients and Strouhal numbers are provided in Table 2for the three levels of grid refinement and time-step resolutions.In the following the velocities are labeled u, v and w for u_1,u_2 and u_3, respectively. Further non-dimensional time-steps $\delta t^* = u\delta t/d$, and velocities e.g. u/u_∞ are used.

Onefundamental problem of a grid convergence study is the rapid growth of computationaldemands that follow from grid refinement. Good practice might be that at least three different grid resolutions, with each having twicethe amount of cells in all directions as its predecessor. In this sense, a gridconverge study has not been performed here. However, three different gridswith successively finer cells have been used. As shown in Table 1 the numberof cells in the span-wise (z) direction was kept unchanged at the second step of refinement. This was also the case for the number of cells in the outer quadrilateral parts of the domain. However,the number of cells was doubled in the grid refinement zone's x,y-plane.

4.1 Global force statistics

Fig. 3 shows a time-history plot of the global lift and drag force coefficients C_l and C_d, respectively. The vertical lines indicate the starting pointof the time-averaging period for the simulation shown. The time averaging period was chosen from a purely visual inspection ofthe drag time history. Within the time averaging period the simulation isseen to be at a reasonably

stable level. The time-averaged coefficients for lift, C_l drag, $C_d$and the root mean square of their fluctuations, i.e.$C_l'$and C_d',as well as the Strouhal numbersSt, are listed in Table 2together with results from published findings. The drag coefficients are a sum of thecontributions from pressure drag and frictiondrag. In the simulation based on grid C the individual contributions were calculated, and the friction drag was found to contribute with less than1% of the total drag. The Strouhal number is based on the peak in thespectrum of the lift force shown in Fig. 4.

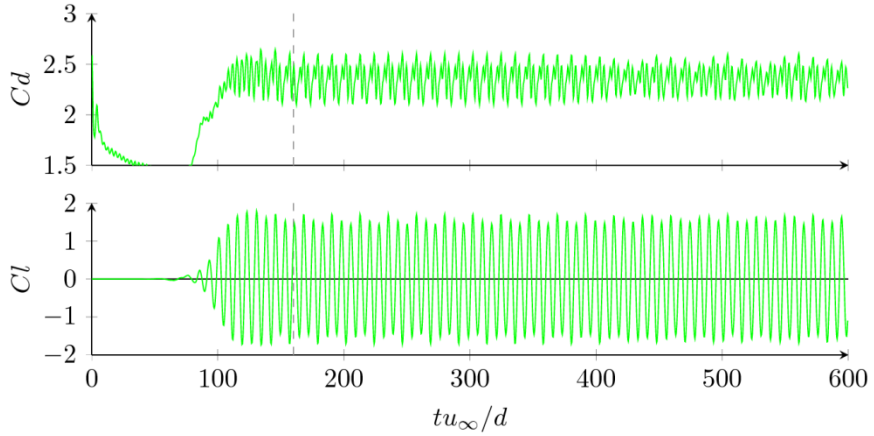

Fig. 3. Non-dimensional time series of the drag and lift coefficients for the present simulations. Here shown for Grid A.

To evaluate grid convergence the global force statistics were comparedfor the three grid resolutions. The results are shown in Table 2.A 5%decrease in time-mean drag can be observed when refining thecoarse grid (grid A) twice to obtain the finest grid (grid C). At the sametime a33% increase in the fluctuating drag $C_d'$and an 22%decrease in the fluctuating lift can be observed accompanied by a 3% decrease in Strouhalnumber. It appears that the Strouhal number is easily predicted, as thethree levels of grids give almost identical results, which are also within theexperimental range. This observation is consistent with the notion of (Rodiet al. 1997), that the Strouhal number was only weakly affected by thecombination of numerical methods. The finer grids give a time-mean dragcoefficient $\bar{C}_d$, that is less than 2% higher than the reported experimental range, and a fluctuating drag coefficient C_d' that is within the reportedexperimental range.
As the rate of change in fluctuating drag from grid B to C (+20%) isactually higher than the change when going from grid A to grid B(+10%),the data does not suggest that the solution has converged. However, both fluctuating lift and time-mean drag have reduced rates of change at the second step of refinement. The fluctuating lift goes from a13% increaseto a 7% increase, while the time-mean drag goes from a 3.4% decrease toa 1.8% decrease. Hence, the latter findings do suggest that the results areconverging. The large change in the fluctuating quantities may be related to the different levels of time steps used. One could speculate that thesmaller time steps caused an increase in the fluctuations, as is the case withthe present data. This issue is addressed in the following.

To investigate temporal convergence, simulations have been carried out with three different time-steps. All three simulations are based on grid B. Againwe use the global force statistics to

evaluate the convergence of the results.Table 2 lists the global force statistics and Strouhal numbers. The Courant-Friedrich-Levi, CFL, condition is enforced in all the simulationsi.e. Courant numbers are kept below 1.0.The non-dimensional time steps used were $\delta t^* = 0.008$; 0.004 and 0.002which resulted in Courant numbers of approximately $Co = 0.5$, 0.25 and 0.125 respectively.An increase in the temporal resolution is seen to cause an increase in the time-meandrag, however the increase in temporal resolution from $\delta t^* = 0.008$ to $\delta t^* = 0.002$only caused a 3% change in the time-mean drag, whileother parameters remained virtually unchanged. Hence, in the following we shall assume that temporal convergence has been reached. We will alsoconclude that the strong changes in the fluctuating drag experienced when refining the grid are caused by the grid, and hence not by the altered time-step.

Source	$\bar{C}_d$	C'_d	C'_l	St
Grid A, $\delta t^* = 0.008$	2.36	0.127	1.12	0.134
Grid B, $\delta t^* = 0.008$	2.24	0.14	1.27	0.134
Grid B, $\delta t^* = 0.004$	2.28	0.14	1.27	0.134
Grid B, $\delta t^* = 0.002$	2.31	0.15	1.26	0.134
Grid C, $\delta t^* = 0.002$	2.24	0.17	1.37	0.130
Grid C, $\delta t^* = 0.002$	$2.07^{(b)}$	$0.16^{(b)}$	$1.27^{(b)}$	$0.125^{(b)}$
Num, (Murakami and Mochida 1995)	2.09	$0.12^{(a)}$	$1.60^{(a)}$	0.132
Num, (Yu and Kareem 1997)	2.14	0.25	1.15	0.135
Num, (Voke 1997), Group NT7	2.05	0.12	1.39	0.131
Num, (Lee and Bienkiewicz 1998)	2.06	0.214	1.214	0.134
Experiments	2.05-2.2	0.17-0.22	1.2-1.32	0.118-0.142

Table 2. Global force coefficients and Strouhal numbers for three different grid resolutions and different time-steps. The listed experimental range is based the published experimental data in (Vickery 1966), (Lee 1975), (Bearman and Obasaju 1982), (Norberg 1993), and (Lyn et al. 1995). Notes:$^{(a)}$ Phase averaged results;$^{(b)}$ blockage corrected using a simplification of (Maskell 1963) shown in (Sohankar et al. 2000).

Grid C was the finest grid used in the current simulations. This grid is seen toreproduce the experimental values very well. The largest deviation fromthe experimental values is approximately 5%. Other values are within thereported experimental range. This level of accuracy is sufficient for civil engineering purposes. The effect of applying blockage corrections is shown in Table 2. The simplified application of (Maskell 1963) in (Sohankar et al.2000) has been used. The blockage correction is given by $\alpha_q = (1 - 1.5\beta)^{-1}$where $\beta$is the blockage ratio, $C_d/C_{d,c} = \alpha_q$and $C'_d/C'_{d,c} = C'_l/C'_{l,c} = \alpha_q$. The Strouhal number was corrected using $St_c = St/\sqrt{\alpha_q}$.Except for theGrid C results in Table 2no blockage correction has been applied to theremaining results presented in the following. This decision was based onthe fact, that the method is yet to be validated for the presentnumerical setup.

The spectral content of the global forces has also been investigated andcompared to the results reported by (Vickery 1966). Fig. 4shows thereduced normalized power spectrum of the lift and drag forces in the case ofsimulation on grid B using $\delta t^* = 0.004$. The lift spectrum is seen to

resemblethe experimental curve obtained by (Vickery 1966). Both the variation(shape) and peak value is in very close agreement; however the peak isshifted slightly towards higher frequencies i.e. a higher Strouhal number isobtained in our simulations. The Strouhal number obtained is still withinthe experimental range, as indicated in Table 2. The shape of the spectrumof the drag force is also seen to be very well resembled, though theenergy seems to be narrower banded in the present simulations. Whencomparing these curves one should keep in mind that the inlet flow in thesimulations was completely turbulence free, whereas some inlet turbulencehas certainly been present in the experiments by (Vickery 1966). Such inletturbulence is likely to be high frequency, and hence one could imaginethis to widen the drag spectrum (distributing energy over a wider rangeof frequencies), and consequently reducing the spectrum peak value. Thespectra's presented was calculated based on Welch's averaged periodogrammethod (Welch 1967) using a hamming window, with a window size ofone quarter of the time signal and the overlap was half the window size.

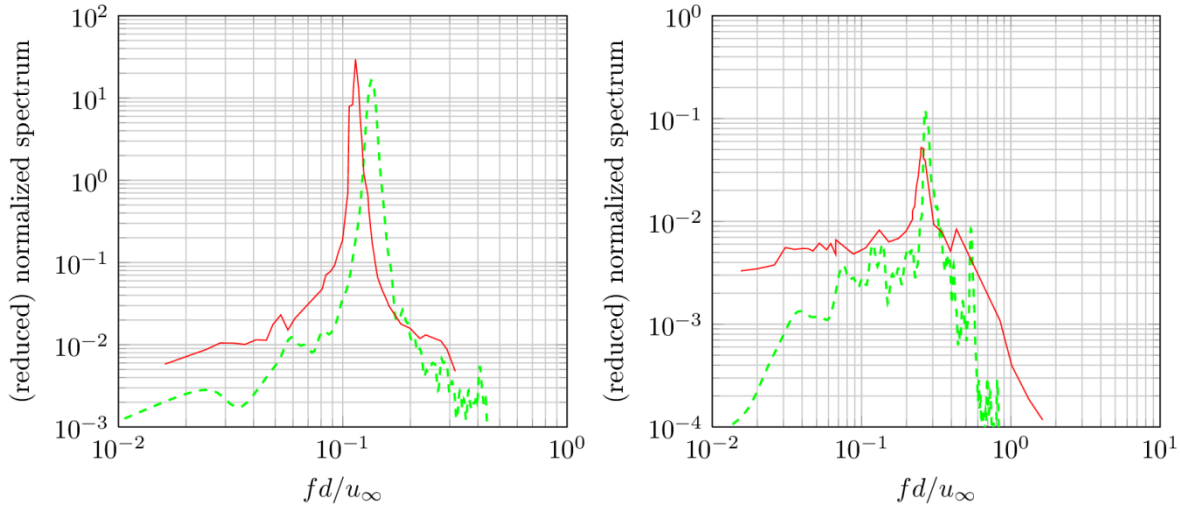

Fig. 4. The reduced normalized spectrum of lift- (left) and drag force (right) coefficients. —, (Vickery 1966); - - -, Present simulations, grid B.

4.1 The velocity field

Velocity profiles may contribute to the understanding of the flow around bluff bodies. In some fields of civil engineering the velocity profiles mighteven be the primary goal. These can for instance be used for comfort studiesaround buildings, or in the evaluation of dispersion of pollutants etc.

In the present work we will include the velocity profiles to ensure that the simulated flow fieldsmatch that of corresponding experiments. The velocity profiles obtained in the present simulations are compared to the results of (Lyn et al. 1995). The data used in the plotare from the ERCOFTAC database. Details of the velocity field are presented at a number of cross flow stations positioned at; $x/d = 0$, $x/d = 0.5$,$x/d = 1.0$ and $x/d = 4.5$. Furthermore, details are given in a stream-wiseline placed in the center of the cylinder $y/d = z/d = 0$.

In the following figures the velocity profiles are shown for the three different simulations in the spatial convergence study. I.e. the velocityprofiles are shown for grid A, B, and C[1].The recirculation length[2] is found to be 1.36, 1.34 for grid A and B, respectively,while (Lyn et al. 1995) reported 1.38. The maximum time-meanreverse velocity in the recirculation zone was found to be -0.183,-0.153 forgrid A and B, respectively, while (Lyn et al. 1995) reported it to be -0.211.The velocity at $(x/d = 10)$ has recovered to$\approx 0.78(0.68$at $x/d = 30)$ and0.64 (0.71 at $x/d = 30$) for grid A and B, respectively. The recirculationlength is well captured with both grid A and B. (Under-predicted by lessthan 3%)

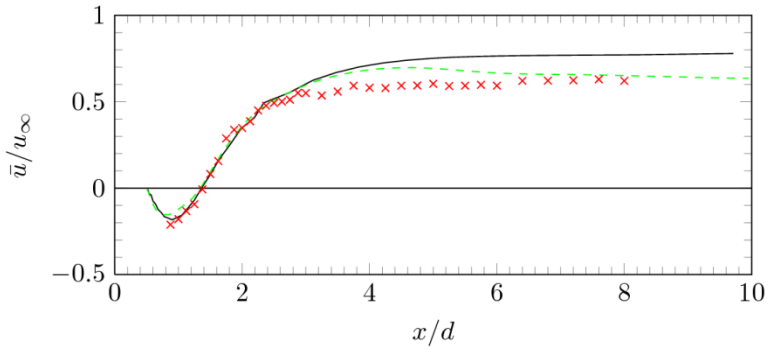

Fig. 5. Time-mean stream-wise velocity.×, (Lyn et al. 1995). Present simulations;—, Grid A; - - -, Grid B.

At first glance of Fig. 5 the prediction of the recovery velocityseems to depend on the resolution of the outer grid, i.e. the successive finergrids provide improved predictions. However, the final recovery velocity at$x/d = 30$ is very similar for the two grids. The simulation based on grid Bseems to shows a peak in the recovery velocity centered around a downstream locationof $x/d \approx 4.0$.However, this "peak" value is slightly lower than the final recovery.The time-mean stream-wise and cross-stream velocities are shown in Fig. 6for each of the four cross-stream locations. Though no quantitativemeasures of divinations have been taken, it seems that refinement of thegrid leads to predictions in better agreement with the experiments. We notethat the simulations provide time-mean velocity profiles which are hardlydistinguishable from the experimental findings.

The fluctuating quantities are given in terms of the Reynolds stresscomponents[3].Fig. 7shows the quantities at the four cross-stream locations. It is obvious that the finer grids, again, provide profiles inbetter agreement with the experimental findings.
Finally, Fig. 8shows the Reynolds stress components measuredin a stream-wise line at $y/d = z/d = 0$. We note again that the finerthe grid, the better agreement with experimental findings. In (Voke 1997)it was noted that the downstream location of the peak of $\overline{v'v'}$ found inthe

[1]The grid C data is unfortunately incomplete due to data corruption during post-processing.
[2]Whenmeasured from $x = 0$.
[3] Or rather the *specific* Reynolds stress components, as they have not been multiplied by the density, ρ. The measurements are basically velocity correlations, but are often referred to as the Reynolds stress. This is due to their general appearance in the Reynolds Averaged Navier-Stokes equations.

numerical simulations, was closer to the cylinder than found in theexperiments. The same tendency can be observed in the data by (Sohankaret al. 2000).

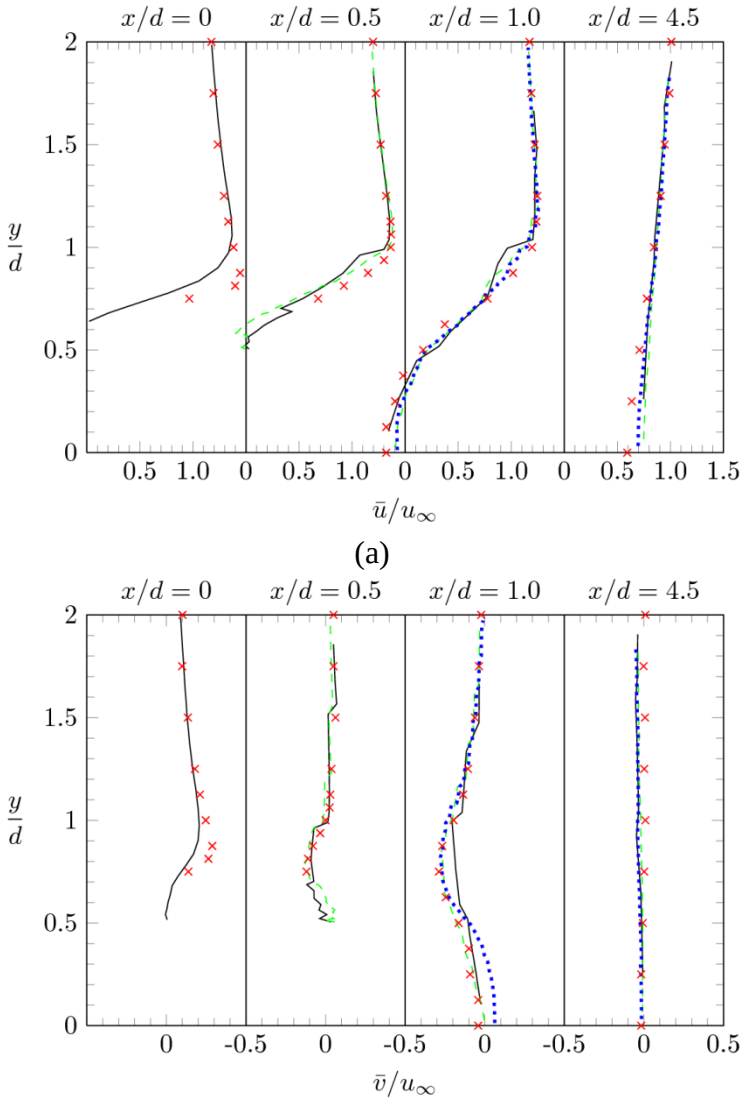

Fig. 6. Time-mean velocity distributions at four cross flow stations. ×, (Lyn et al. 1995). Present simulations: —, Grid A; - - -, Grid B; ·····, Grid C. (a) is the stream-wise velocity $\bar{u}$; (b) is the cross-stream velocity $\bar{v}$.

The present data seems to support the experimental findings.Overall, the velocity distributions, including their fluctuating quantities,have shown close agreement with experimental findings. Refinement of thegrid has led to better agreement with experimental findings, especiallyfor the fluctuating quantities. In regard of convergence of the results, itseems that (without quantitative measures to support this) the results areconverging.

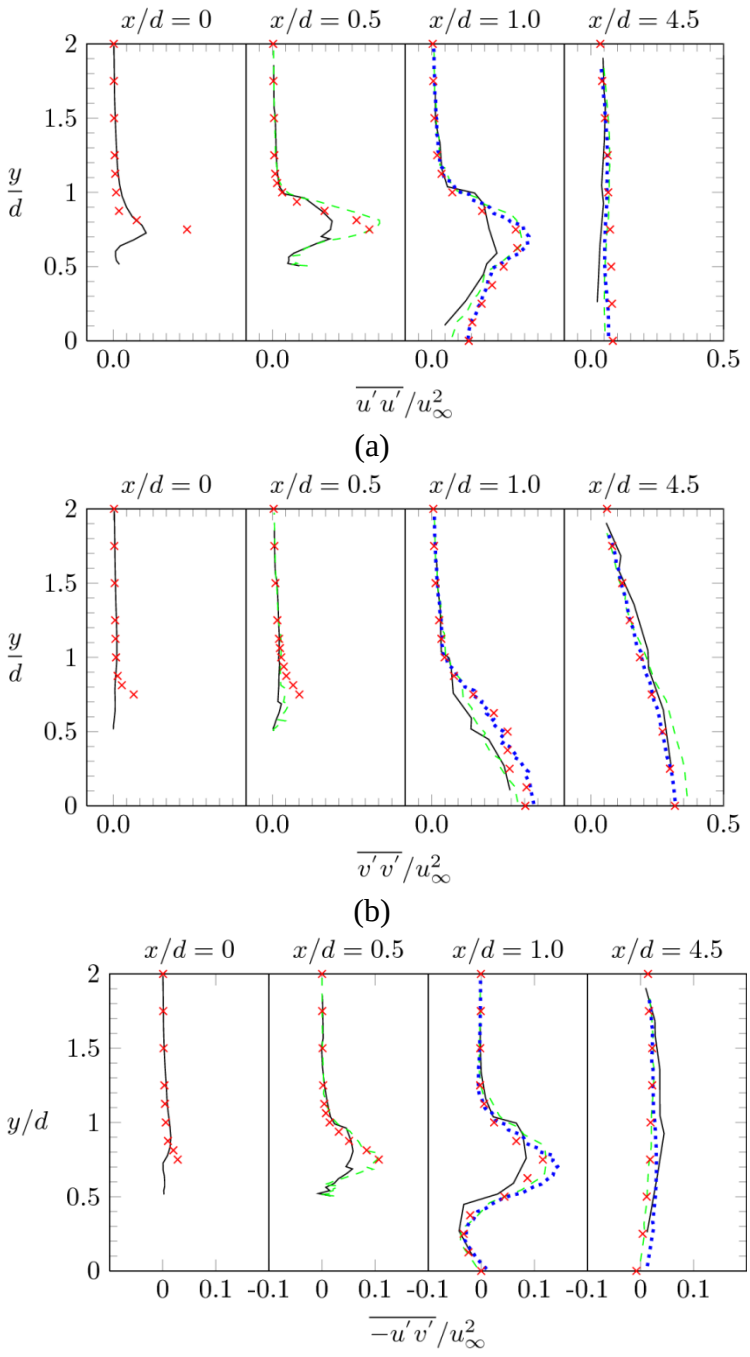

Fig. 7. The Reynolds stress terms at four cross flow stations. ×, (Lyn et al. 1995). Present simulations: —, Grid A; - - -, Grid B; ·····, Grid C. (a) is the u' component; (b) is the v'component; (c) is the cross correlation between u' and v'.

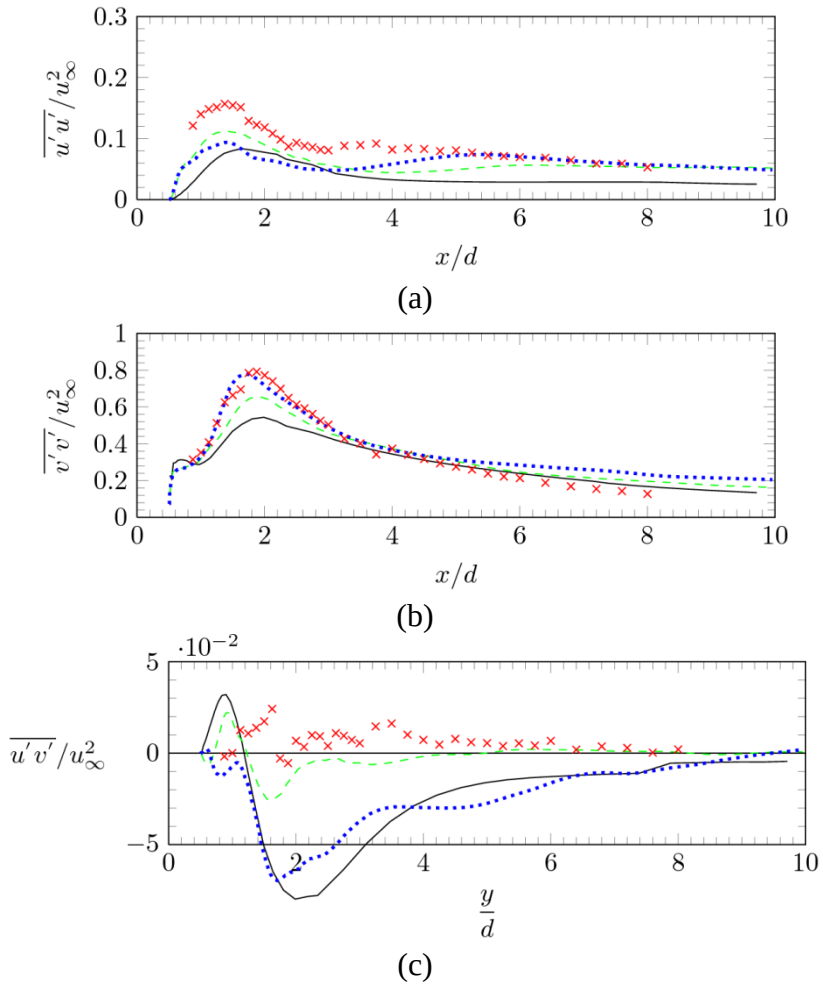

Fig. 8. The Reynolds stress terms in a stream-wise line through the cylinders center of gravity. ×, (Lyn et al. 1995). Present simulations: —, Grid A; - - -, Grid B; ·····, Grid C. (a) is the u' component; (b) is the v'component; (c) is the cross correlation between u' and v'.

4.2 Surface pressure statistics

Here we will present the pressure distributions as time-mean local pressurecoefficients C_p. The pressure distributions will be compared to the experimentsby (Lee 1975) and (Bearman and Obasaju 1982). The fluctuating pressure coefficients C_p' are also presented. The time-mean pressure distributionsobtained in the numerical simulations have been corrected, so that$C_p = 1.0$at the front center surface.The time-mean pressure distributions are given in Fig. 9. Thesharp corner points of the square pose a problem in the numerical simulations.The singularities here cause the pressure readings to deviate substantially.As the grid is refined this effect is minimized. Using the coarsegrid leads to a pressure distribution that deviate slightly (say 5-10%) on thetop and bottom surfaces of the cylinder. However, as the grid was refinedthe pressure distributions are found to be between the two experiments.

Fig. 10 shows the fluctuating pressure coefficients. Thesehave been reported to vary significantly between individual windtunnel experiments. With the present simulations the coarse grid shows alower fluctuating pressure coefficient on the top and bottom sides of

thecylinder than shown in the experiments.As the grid is refined the fluctuating pressure coefficient increases. This is consistent with the increase in the fluctuating lift force coefficient during grid refinement (see Table 2).

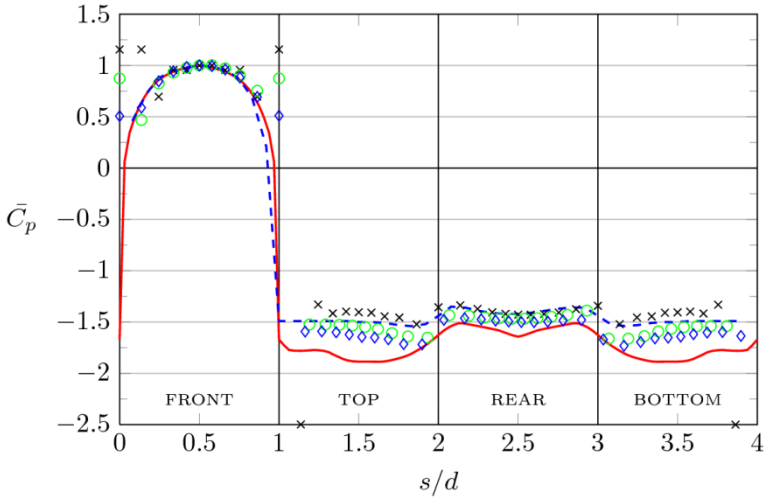

Fig. 9. Time-mean surface pressure coefficient. ——, (Bearman 1982); - - -, (Lee 1975). Numerical: ×, Grid A; ○,Grid B (each 2nd point); ◇,Grid C(each 4th point).

The finer grids show a variation of the fluctuating pressure coefficient thatlies within the two experimental findings used for comparison here. Forcomparison the distribution reported by (Yu and Kareem 1997) has beenincluded in the plot.

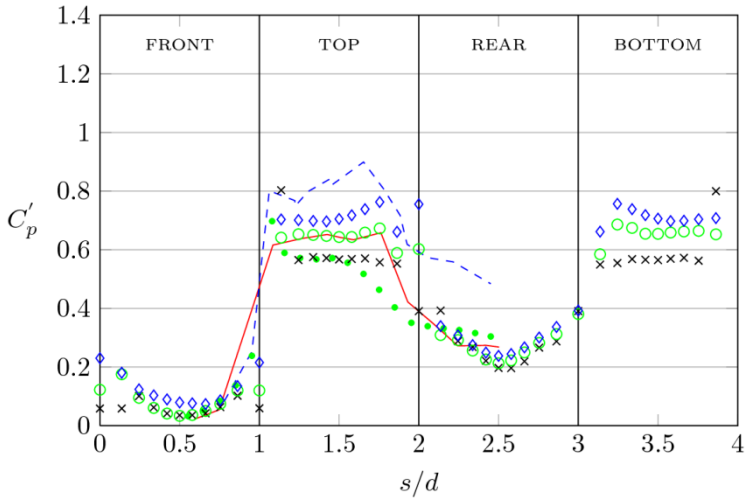

Fig. 10. Fluctuating surface pressure coefficients (rms of pressure fluctuation). ——, (Bearman and Obasaju 1982); - - -, (Pocha 1971). Numerical: ×, Grid A; ○, Grid B (each 2nd point); ◇, Grid C (each 4th point); ·, (Yu and Kareem 1997).

The correlation of surface pressures is essential in the task of estimatingglobal loads from local pressure distributions. It is due to the lack offull correlation that building codes provide smaller shape factors, and henceloads, for large surface areas, than for small areas. For instance

individualcladding elements on a building should be designed for a higher local surfacepressure than the supporting frames that carry a large assembly of claddingelements and thus loads from a large area.

For the present simulations, the correlation of pressures in a cross section near the mid span has beeninvestigated. A base point was chosen on the top surface $5/12\ d$downstreamof the leading edge. The correlation of pressure between this point, andall other points in the cross section was then determined, and plotted inFig. 11. The simulated correlations found with Grid A, appear to bein close agreement with the experimental findings.

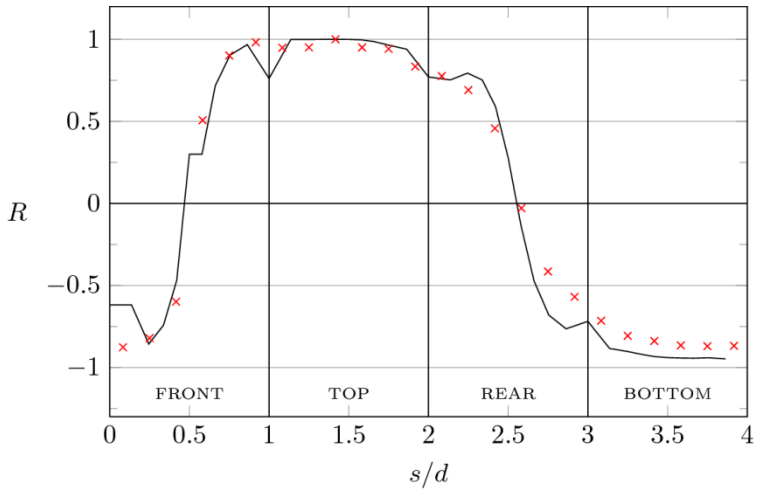

Fig. 11. Circumferential correlation of surface pressures with respect to a pressure tab at the top surface, placed $5/12d$ downstream from the front surface. —, (Lee 1975); ×, Grid A.

5. CONCLUSION

The present test case has shown that the model can in fact simulate the flow around a square cylinder with results that are comparable or improved in comparison to the results of LES simulations. The SMoM model is thus found to provide an alternative to LES.

The SMoMmodel is still immature in comparison to LES models, and does still bear the flow dependent scale parameter$b$. Thus, work is still need to address the general applicability of the SMoM model for civil engineering flows.

REFERENCES

Bearman, P. W. and Obasaju, E. D. (1982).“An experimental study of pressure fluctuations on fixed and oscillating square-section cylinders”.Journal of Fluid Mechanics, **119**(-1):297-321.

Johansson, J. (2011),*Wind loads on structures*, Ph.D. thesis, Institute of Technology and Innovation, University of Southern Denmark. (Pending publication)

Lee, B. E. (1975). “The effect of turbulence on the surface pressure field ofa square prism”. Journal of Fluid Mechanics, **69**(02):263-282.

Lee, S. and Bienkiewicz, B. (1998).“Finite element implementation of largeeddy simulation for separated flows”. Journal of Wind Engineering andIndustrial Aerodynamics, **77-78**:603-617.

Lyn, D. A., Einav, S., Rodi, W., and Park, J.-H. (1995). “A laser-dopplervelocimetry study of ensemble-averaged characteristics of the turbulentnear wake of a square cylinder”. Journal of Fluid Mechanics, **304**(-1):285-319.

Maskell, E. C. (1963). “A theory of the blockage effects on bluff bodies and stalled wings in a closed wind tunnel”. Aeronautical Research Council Reports and Memoranda 3400, Aeronautical Research Council.

Murakami, S. and Mochida, A. (1995).“On turbulent vortex shedding flow past 2d square cylinder predicted by CFD”. Journal of Wind Engineering and Industrial Aerodynamics, **54-55**:191-211. Third Asian-Pacific Symposium on Wind Engineering.

Nikuradse, J. (1932). ”Gesetzmässigkeiten der turbulentenStrömung in glattenRohren : mit 9 Zahlentafeln”. *Beil. zuForschungauf d. Gebiete d. Ingenieurwesens; Ausg. B, Bd. 3, Septemper/Oktober, VDI-Forschungsheft 356*. VDI-Verl. Zugl.: Göttingen, Kaiser-Wilhelm-Inst., Diss., 1932.

Nielsen, M.P., Shui, Wan, Petersen, Ulrik E. 2006. *Turbulence model*. Unpublished. A draft is available with the authors.

Norberg, C. (1993). “Flow around rectangular cylinders: Pressure forces and wake frequencies”. Journal of Wind Engineering and Industrial Aerodynamics,**49**(1-3):187-196.

Rodi, W., Ferziger, J., Breuer, M., and Pourquie, M. (1997). “Status of large eddy simulation: Results of a workshop”. Journal of Fluids Engineering,Transactions of the ASME, **119**(2):248-262.

Sohankar, A., Davidson, L., and Norberg, C. (2000). “Large eddy simulation of flow past a square cylinder: comparison of different subgridscale models”. Transactions of the ASME. Journal of Fluids Engineering,**122**(1):39-47.

Vickery, B. J. (1966). “Fluctuating lift and drag on a long cylinder of square cross-section in a smooth and in a turbulent stream”. Journal of Fluid Mechanics, **25**(03):481-494.

Voke, P. R. (1997). “Flow past a square cylinder: Test case LES2”. InJ.-P.Chollet, P. R. V. and Kleiser, L., editors, *Direct and Large Eddy Simulation II*, ERCOFTAC Series, pages 355-373.

Welch, P. (1967). “The use of fast fouriertransform for the estimation of power spectra: A method based on time averaging over short, modifiedperiodograms”. *IEEE Transactions on Audio Electroacoustics*, AU-15:70-73.

Yu, D.-h.and Kareem, A. (1997). “Numerical simulation of flow aroundrectangular prism”. Journal of Wind Engineering and Industrial Aerodynamics,**67-68**:195-208.